REVISTAS CIENTÍFICAS INDEXADAS
BISTUA
FACULTAD DE CIENCIAS BÁSICAS - UNIVERSIDAD DE PAMPLONA
fcb Facultad de Ciencias Básicas Universidad de Pamplona

BISTUA ***Rev. FCB, Volumen 22 (2) (2024). Pamplona-Colombia.***
https://doi.org/10.24054/bistua.v22i2.2645

A case study of PT pseudosections constructed in the MnNCKFMASH ($MnO-Na_2O-CaO-K_2O-FeO-MgO-Al_2O_3-SiO_2-H_2O$) system for metapelitic rocks in the garnet zone of the Silgará Formation, southwestern Santander Massif (Colombia)

Estudio de caso de seudosecciones PT construidas en el sistema MnNCKFMASH ($MnO-Na_2O-CaO-K_2O-FeO-MgO-Al_2O_3-SiO_2-H_2O$) para rocas metapelíticas en la zona de granate de la Formación Silgará, en el Macizo de Santander suroccidental (Colombia)

Paula Giovanna Delgado G. [a]**; Ana Milena Suárez A.** [a]**; Carlos Alberto Ríos-Reyes** [a*]; **Julián Andrés López I.**[b]**; Oscar Mauricio Castellanos A.**[c]

[a] *Universidad Industrial de Santander, Escuela de Geología, Bucaramanga, Colombia; paulagalvisgeo@gmail.com; aniitasuarez20@gmail.com.*
[b] *Universidad Nacional de Colombia, Departamento de Geociencias, Bogotá, Colombia; jalopezi.uis@gmail.com*
[c] *Universidad de Pamplona, Facultad Ciencias Básicas, Villa del Rosario, Colombia; oscar.castellanos@unipamplona.edu.co*

Correspondencia*: paulagalvisgeo@gmail.com*

Recibido*: Diciembre 05, 2023.* ***Aceptado****: Julio, 15 2024.* ***Publicado****: Agosto, 21 2024.*

Abstract

This study examines the metamorphic evolution of metapelitic rocks in the garnet zone of the Silgará Formation, located in the southwestern Santander Massif, Colombia. Utilizing advanced thermobarometric methods and detailed mineralogical analysis, PT pseudosections were constructed in the MnNCKFMASH system, informed by bulk rock and mineral chemistry data. Computer programs such as THERIAK/DOMINO, GTB, and GIBBS were employed to estimate maximum PT conditions of metamorphism and delineate metamorphic PT paths. The pseudosections confirm previously published PT conditions (495-518 °C and 4.4-5.5 kbar) for the garnet zone, indicating a stable mineral assemblage of garnet, potassium feldspar, biotite, muscovite, and quartz. The study also identifies retrograde metamorphism through mineral reactions such as the formation of chlorite from biotite and garnet, sericite from plagioclase, and chlorite + sericite from staurolite. These reactions suggest decompression under lower PT conditions with high H2O levels. This research enhances the understanding of the region's geological history, emphasizing the role of advanced thermobarometric techniques and detailed mineralogical studies in elucidating complex tectono-metamorphic processes.

Keywords**:** garnet zone; Silgará Formation; southwestern Santander Massif; PT pseudosections; thermobarometry.

Resumen

Este estudio examina la evolución metamórfica de las rocas metapelíticas en la zona de granate de la Formación Silgará, ubicada en el suroeste del Macizo de Santander, Colombia. Utilizando métodos termobarométricos avanzados y análisis mineralógicos detallados, se construyeron pseudosecciones PT en el sistema MnNCKFMASH, basadas en datos de química de roca y mineral. Se emplearon programas informáticos como THERIAK/DOMINO, GTB y GIBBS para estimar las condiciones máximas de PT del metamorfismo y delinear las trayectorias PT metamórficas. Las pseudosecciones confirman las condiciones de PT previamente publicadas (495-518 °C y 4.4-5.5 kbar) para la zona de granate, indicando una paragénesis mineral estable de granate, feldespato potásico, biotita, moscovita y cuarzo. El estudio también identifica el metamorfismo retrógrado a través de reacciones minerales como la formación de clorita a partir de biotita y granate, sericita a partir de plagioclasa, y clorita + sericita a partir de estaurolita. Estas reacciones sugieren una descompresión bajo condiciones de PT más bajas con altos niveles de H2O. Esta investigación mejora la comprensión de la historia geológica de la región, enfatizando el papel de las técnicas termobarométricas avanzadas y los estudios mineralógicos detallados en la elucidación de procesos tectono-metamórficos complejos.

Palabras clave**:** zona de granate; Formación Silgará; Macizo de Santander suroccidental; seudosecciones PT; termobarometría.

1. Introduction

The development of large thermodynamic datasets, including properties for metapelitic rock-forming minerals, allows the calculation of stability limits for minerals and mineral assemblages in PT space. This calculation is typically performed in relatively simple chemical systems with a

limited number of phases considered [1]. The estimation of pressure-temperature-time (PTt) history of metapelitic rocks and the constraints in the reconstruction of their tectono-metamorphic evolution in different tectonic regimes have been of interest in metamorphic petrology for a long time [2]. The quality of the internally consistent thermodynamic dataset of mineral end-member properties has improved considerably in recent years [3-5]. The model system KFMASH (K_2O-FeO-MgO-Al_2O_3-SiO_2-H_2O) has been studied intensively in order to develop petrogenetic grids for the range of common mineral assemblages in metapelitic rocks [6]. Early qualitative grids were based on natural mineral paragenesis [7-8]; later quantitative grids were based on internally-consistent thermodynamic data sets [9-10]. In recent years a number of studies have been carried out to augment the system with additional components such as Na_2O, CaO, TiO_2, Fe_2O_3 and MnO [11-12]. According to Horváth [6], from these components MnO has the most important role in stabilizing ferromagnesian minerals, mostly garnet. Therefore, the chemical system appropriate for quantitative modeling of any particular rock is dictated by mineralogy and bulk rock composition, and ignoring elements that affect mineral stability degrades the applicability of quantitative phase equilibria modeling to real rocks [1]. The purpose of this work is to establish the metamorphic PT conditions from selected samples of metapelitic rocks of the Silgará Formation´s metamorphic zones, using different thermobarometric methods including pseudosections constructed using THERMOCALC version 3.26 [13] and thermodynamic data of Holland and Powell [4], THERIAK/DOMINO version 01.08.09 [14], and GTB version 30.03.06 [15], and Gibbs [16]. Particularly, the more recent application of pseudosections to metapelitic rocks offers a possibility to reconstruct the PT path for such rocks.

2. Geological setting

The NW-SE trending Santander Massif is situated in the Eastern Cordillera of the Colombian Andes, where it is split into the NNE-SSW trending Perijá Range in Colombia and the ENE-WSW trending Mérida Andes in Venezuela (Figure 1). However, the Eastern Cordillera and the Mérida Andes do not have a direct genetic relationship between them; they are separated by the southern termination of the left-lateral strike-slip Santa Marta - Bucaramanga Fault system and the Santander Massif [17]. According to Jimenez *et al*. [18], the Bucaramanga - Santa Marta Fault system juxtaposes metamorphic basement rocks to the east and sedimentary Jurassic to Cenozoic rocks to the west, and it can be divided along strike into three major zones (Northern, Central, and Southern zone), where it bounds several distinct geological provinces. The complex metamorphic basement of the Santander Massif can be divided into the following geological units (in ascending order of tectono-stratigraphic level): Bucaramanga Gneiss Complex, Silgará Schists Formation, Chicamocha Schists Formation, Orthogneiss, and San Pedro Phyllites Formation [19-20], all of which are cut by intrusive rocks that recorded magmatic events of Caledonian to Jurassic age [21-26]. Mantilla *et al*. [27] reported U-Pb ages from detrital zircons of ~900 Ma (Neo-Proterozoic) for the Silgará Schists Formation and ~500 Ma (Middle Cambrian age) for the Chicamocha Schists Formation. They suggest that the climax of the metamorphism that affected these metamorphic units occurred during the main event of the Fammatinian orogeny (Early Ordovician; 480-470 Ma), which can be related to the emplacement of syn-tectonic granitoids of 480-472 Ma that form part of the Orthogneiss [28]. The San Pedro Phyllites Formation represents the youngest metamorphic unit in the Santander Massif (more than 450 Ma - Late Ordovician), which was affected by a metamorphic event that can be related to a minor event of the Fammatinian orogeny [27], producing very low-grade metamorphic rocks (mainly phyllites). The Bucaramanga Gneiss Complex consists of pelitic gneisses, with minor amounts of amphibolites and orthogneisses, which were metamorphosed to high temperatures as they are in part migmatitic [19]. Despite the subdivision proposed by Mantilla *et al*. [20] for the Silgará Formation, we will keep this denomination in the present study referring to the rocks that emerge in the SWSM. The prevailing rocks of the Silgará Formation correspond to metapelitic rocks, with minor intercalations of metamafic rocks, which display a well-developed schistosity. Schäfer *et al*. [29] studied the petrology and geochemistry of the metamafic rocks and propose a magmatic origin for them, representing sills emplaced prior to deformation and metamorphism. The Orthogneiss generally show similar foliation and lineation with those of the surrounding Bucaramanga Gneiss Complex and Silgará Formation metamorphic rocks. The basement of the Santander Massif is unconformably covered by a sedimentary sequence of Devonian to Tertiary age [19]. During the last decades, the metapelitic sequence at the Santander Massif has been the focus of interest in several studies [20,27,29-37-45], which mostly were directed towards the estimation of metamorphic PT conditions. The Silgará Formation cropping out in the southwestern Santander Massif (SWSM) (Figure 1) is mainly composed of metapelitic rocks, with minor intercalations of metamafic rocks (sills emplaced prior to deformation and metamorphism) that generally strike NW–SE and dip to the SW and have been affected by multiple deformations, giving rise to interference patterns [38]. These rocks display a well-developed schistosity, though sedimentary bedding is locally preserved and well displayed in the lowest-grade metamorphic rocks. According to Ríos [31], the lithology of this metapelitic sequence changes in composition northeastward from quartz-rich pelitic schists (southwest) to feldspar-rich semipelitic schists (northeast). The Silgará Formation in the SWSM was probably affected by Caledonian regional metamorphism [38]. The classic scheme of metamorphic zones and isograds of the Silgará Formation suggested by Ward *et al*. [19-20,46-47] has been modified by previous studies [31,38], revealing not only a sequence of metamorphic zones (chlorite, biotite, garnet, garnet-

staurolite, staurolite-kyanite, and sillimanite) but also its complex history of metamorphism and deformation. The regional metamorphic grade of the Silgará Formation rocks decreases southwestward from the sillimanite zone to the chlorite zone. Metamorphism has occurred under low- to high-temperature and medium-pressure conditions (Barrovian-type metamorphism) and reflects the high heat flow in this part of the Santander Massif [38]. During the tectono-metamorphic evolution, these rocks were tectonically transported to lower crustal levels up to reach the baric peak conditions, which was followed by decompression and a slight increase of temperature up to the thermal peak conditions [31]. The retrograde metamorphism was characterized by decompression and cooling.

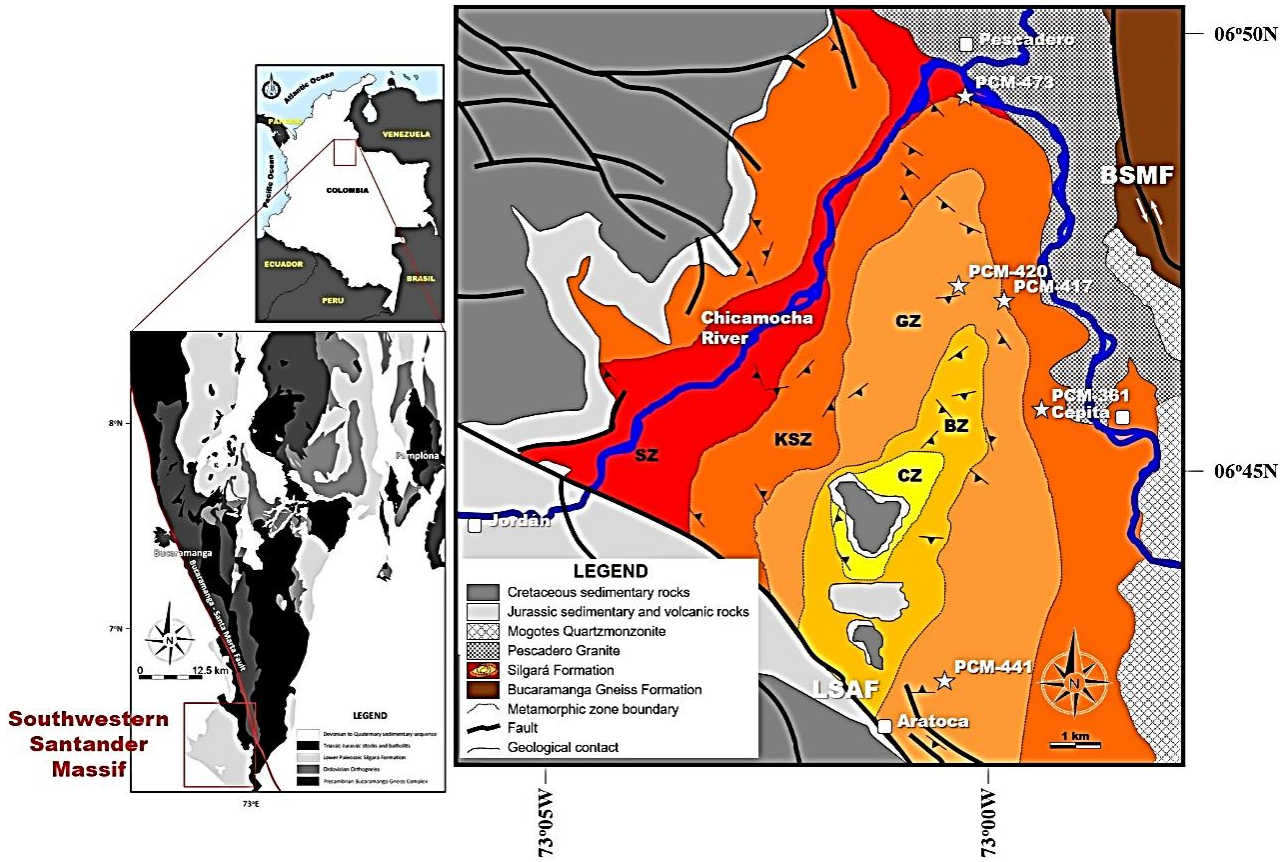

Figure 1. Left, Santander Massif, showing the distribution of the Silgará Formation at the SWSM (adapted and modified after Goldsmith *et al*. [21]. Right, regional thermal structure of the Silgará Formation in the SWSM has been suggested by previous studies [19-20,38,46-47] on the basis of field observations and petrographic analysis, with the following metamorphic zones: chlorite (CZ), biotite (BZ), garnet (GZ), kyanite-staurolite (KSZ) and sillimanite (SZ). Fuente: Autor(es).

3. Materials and methods

Sample locations within the Silgará Formation at the SWSM are given in the geological sketch map of Figure 1. Detailed petrographic studies of three thin sections (labeled as PCM-417, PCM-420 and PCM-441) were carried out. The rocks of interest in this study, which correspond to metapelitic rocks, were selected based on the information available on total rock and mineral chemistry, as well as on the programmed character of their chemical zoning. The main petrographic aspects of the Silgará Formation metapelitic rocks are shown in Figures 2-4. Whole-rock chemistry of metapelitic rocks were performed on powder pellets with a BRUKER Wavelength Dispersive X-ray Fluorescence (WDXRF) spectrometer S8 TIGER, which is fitted with an end window X-ray tube with Rh-target and a 10-position beam filter changer allowing excitation conditions to be easily adjusted to achieve optimum results. Samples milled in an agate mortar and then sieved to a size less than 38 µm. Then, they calcined to 950 °C for 2 hours with a heating rate of 200 °C/hour for determining the loss on ignition. The calcined samples again milled and then added in a sample holder (plastic cup of 34 mm diameter) for measurement. The spectra and the concentrations obtained were analyzed using the QUANT-EXPRESS software and the Fundamental Parameter method whose detection limits reach element concentrations mg/kg. Electron microprobe analyses were performed using a JEOL JXA 8800M electron probe microanalyzer at the Research Center for Coastal Lagoon Environments, Shimane University (Japan), under the following analytical conditions: 15 kV accelerating voltage and 2.4×10^{-8}A probe current. Data acquisition and reduction were carried out using ZAF correction procedures. Natural

and synthetic minerals were used as standards. Mineral compositions were determined by multiple spot analyses.

4. Results

4.1. Petrography

The analyzed samples exhibit petrographic evidence of textures and structures indicative of mineral equilibrium, which are comprehensively described below. This aspect is of paramount importance as it offers crucial insights into the metamorphic evolution and conditions of metapelitic rocks in the garnet zone of the Silgará Formation, located in the southwestern Santander Massif (Colombia). The detailed examination of textures and structures in mineral equilibrium not only aids in understanding the geological history of the region but also forms a fundamental basis for constructing PT pseudosections in the MnNCKFMASH system. These pseudosections, in turn, play a crucial role in estimating peak metamorphic conditions and identifying metamorphic pathways, thereby providing a comprehensive framework for studying the metamorphic evolution within the specific context of the Silgará Formation. Sample PCM-417 represents a micaceous schist characterized by a high content of biotite, garnet, plagioclase, quartz, muscovite, and chlorite. The rock exhibits polygonal aggregates, accompanied by triple points, and mineral growth in microlithons. It displays granolepidoblastic textures, with localized occurrences of porphyroblastic and poikiloblastic textures. The cleavage domain is wide, zonal, and parallel. Additionally, cataclastic textures are locally observed, indicating a brittle deformation process (Figure 2). Retrograde metamorphism is evidenced by chlorite after garnet and biotite, as well as sericite after plagioclase. Veinlets of epidote crosscut the main foliation of the rock. Garnet porphyroblasts, projecting into a matrix rich in quartz and plagioclase, exhibit hypidioblastic outlines, high relief, and pale color. They display a poikiloblastic texture and are randomly distributed within quartz and plagioclase-rich bands, with inclusions of minerals from the surrounding matrix. Biotite, marking the cleavage domain, shows hypidioblastic and xenoblastic outlines, a broadleaf habit, and greenish-brown pleochroism. It grows as microlithons in contact with quartz and plagioclase, with alteration to chlorite evident. Muscovite displays hypidioblastic and xenoblastic outlines, very low relief, and high interference colors. Quartz exhibits homeoblastic to heteroblastic and xenoblastic outlines, with wavy extinction in some crystals, found in aggregates resulting from static recrystallization, forming a foam structure. Plagioclase presents homeoblastic to hypidioblastic outlines, colorless or pale brown coloration, and tabular habit, developing polygonal aggregates. Chlorite displays heteroblastic and xenoblastic outlines, with mild pale green pleochroism and anomalous interference colors. Accessory minerals include tabular ilmenite elongated in the direction of foliation, and small pinhead-like apatite crystals, colorless and standing out above the other minerals. The mineral assemblage of this rock is biotite + muscovite + garnet + quartz + plagioclase, typical of the garnet zone and the green schist facies.

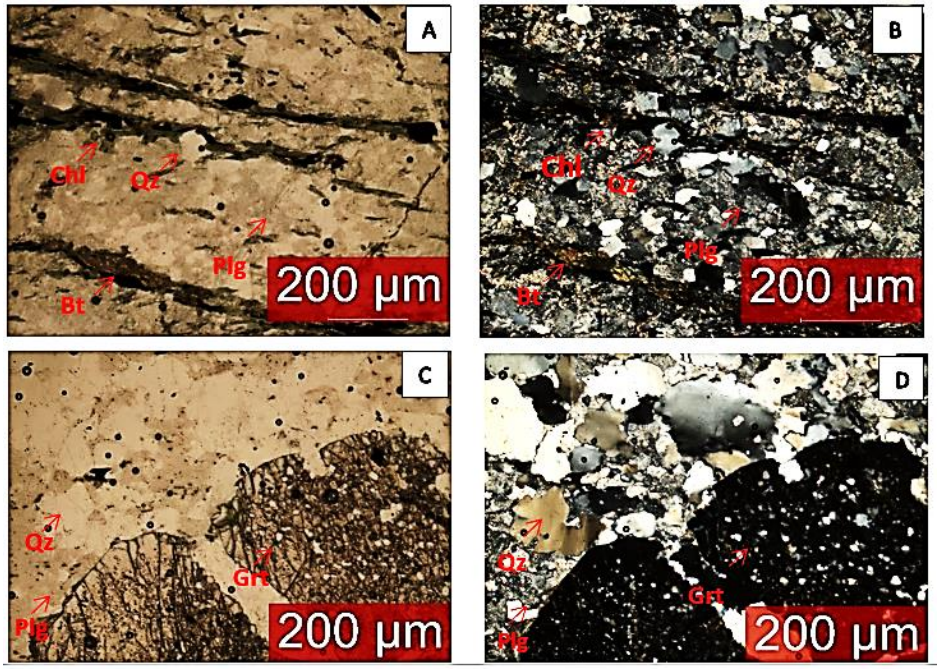

Figure 2. Photomicrographs of the main microstructural and textural features of sample PCM-417. (A)-(B) Granolepidoblastic texture with polygonal aggregates, triple points and mineral growth in microlithons. Wide, zonal and parallel cleavage domain. PPL and XPL, respectively. (C)-(D) Porphyroblastic and poikiloblastic textures. PPL and XPL, respectively. PPL, plane polarized light; XPL, cross polarized light. Qz, quartz; Grt, garnet; Chl, chlorite; Bt, biotite; Mg, magnetite; Plg, plagioclase. Fuente: Autor(es).

Sample PCM-420 is a micaceous schist with a high content of biotite, garnet, plagioclase, quartz, muscovite, and chlorite. It exhibits polygonal aggregates, accompanied by triple points, and mineral growth in microlithons. The rock displays granolepidoblastic textures and locally porphyroblastic textures. The cleavage domain is wide, zonal, and parallel. Locally, cataclastic textures are observed, indicating a fragile deformation process (Figure 3). Retrograde metamorphism is evidenced by chlorite after garnet and biotite, and sericite after plagioclase. Garnet porphyroblasts, projecting into a quartz and plagioclase-rich matrix, show hypidioblastic outlines, high relief, and pale color. They exhibit a poikiloblastic texture and are randomly distributed within quartz and plagioclase-rich bands of the rock, with inclusions of minerals from the surrounding matrix. Fractures filled by chlorite suggest an incipient alteration to this mineral. Biotite displays hypidioblastic and xenoblastic outlines, a broadleaf habit, remarkable greenish-brown pleochroism, and marks the cleavage domain. It grows as microlithons in contact with quartz and plagioclase, with alteration to chlorite evident. Muscovite exhibits hypidioblastic and xenoblastic outlines, very low relief, and high interference colors. Quartz shows homeoblastic to heteroblastic and xenoblastic outlines, colorless, low relief, and low interference colors, associated with plagioclase, biotite, and garnet. Some quartz crystals have wavy extinction and are found in aggregates with a foam structure. Plagioclase presents homeoblastic and hypidioblastic outlines, colorless or pale brown coloration, with low interference colors, and tabular habit, developing polygonal aggregates. It lacks twinning due to alteration to sericite, giving it a chalky appearance. Chlorite shows heteroblastic and xenoblastic outlines with mild pale green pleochroism and typical anomalous interference colors. Accessory minerals include abundant tabular ilmenite elongated in the direction of the foliation, suggesting the presence of carbonate-sulphide-rich fluids [48]. The mineral assemblage of this rock corresponds to biotite + muscovite + garnet + quartz + plagioclase, typical of the garnet zone and the green schist facies.

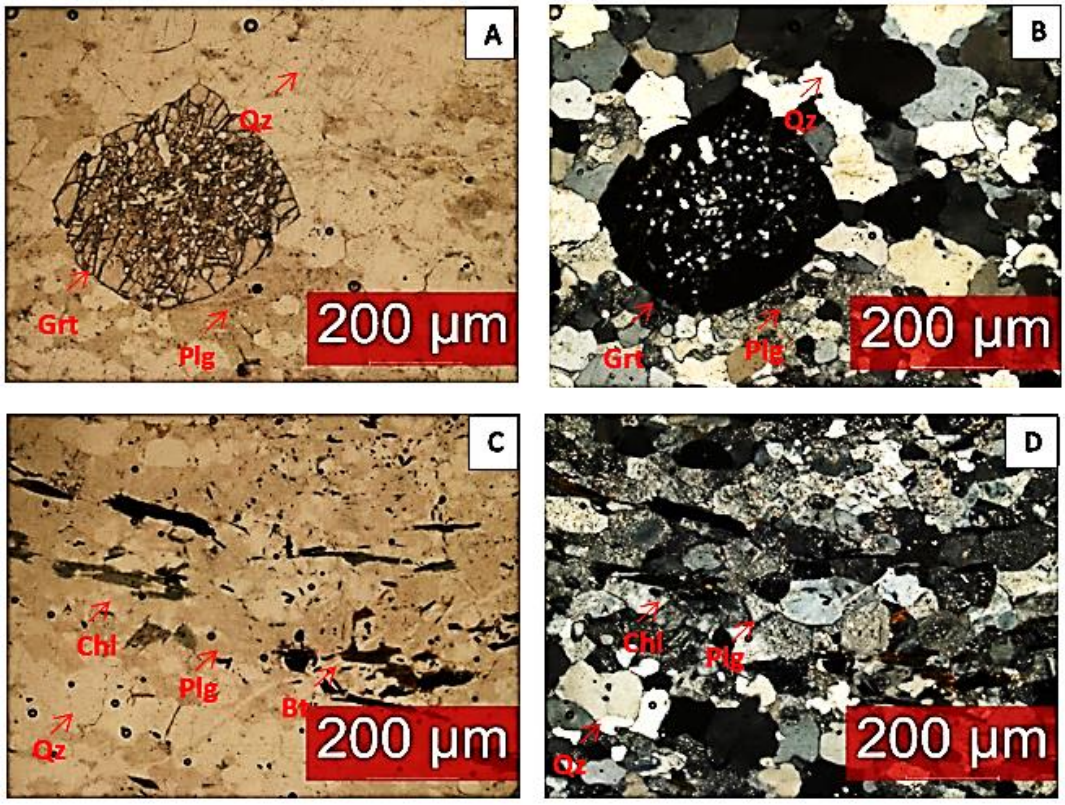

Figure 3. Photomicrographs of the main microstructural and textural features of PCM-420 sample. (A)-(B) Porphyroblastic and poikiloblastic textures. PPL and XPL, respectively. (C)-(D) Granolepidoblastic texture with polygonal aggregates, triple points and mineral growth in microlithons. Wide, zonal and parallel cleavage domain. PPL and XPL, respectively. PPL, plane polarized light; XPL, cross polarized light. Qz, quartz; Grt, garnet; Chl, chlorite; Bt, biotite; Mg, magnetite; Plg, plagioclase. Fuente: Autor(es).

Sample PCM-441 is a micaceous schist composed primarily of muscovite, biotite, garnet, plagioclase, and quartz. It exhibits a well-defined schistosity due to the orientation of muscovite and biotite. The rock shows polygonal aggregates, accompanied by triple points, and mineral growth in microlithons. It displays granolepidoblastic textures and locally porphyroblastic and lepidogranoblastic textures. The cleavage domain is wide, zonal, and parallel. Locally, cataclastic textures are observed, indicating a fragile deformation process (Figure 4). Retrograde metamorphism is

evidenced by chlorite after biotite and sericite after plagioclase. Very fine-grained garnet porphyroblasts exhibit a heteroblastic outline, high relief, and pale color. They are randomly distributed within muscovite-biotite-rich bands and contain inclusions of ilmenite. Fractures filled by chlorite suggest an incipient alteration to this mineral. Biotite displays a homeoblastic to heteroblastic and idioblastic outline, a broadleaf habit, excellent exfoliation, and remarkable brown pleochroism. It marks the cleavage domain of the rock and also grew in a different direction, approximately 30o with the main foliation of the rock. It is associated with muscovite and garnet and shows incipient alteration to chlorite. Muscovite exhibits a heteroblastic to hypidioblastic outline, very low relief, and high interference colors, marking the cleavage domain of the rock and associated with biotite and garnet. Quartz shows a heteroblastic to xenoblastic outline, colorless, low relief, and low interference colors, randomly distributed in the rock and associated with plagioclase, biotite, muscovite, and garnet. Plagioclase displays a heteroblastic and xenoblastic outline, colorless, with low interference colors, without twinning, and associated with quartz, biotite, muscovite, and garnet. Chlorite shows a heteroblastic and xenoblastic outline with mild pale green pleochroism and typical anomalous interference colors, randomly distributed in the rock and associated with quartz, plagioclase, and muscovite. The mineral assemblage of this rock corresponds to biotite + muscovite + garnet + quartz + plagioclase, typical of the garnet zone and the green schist facies.

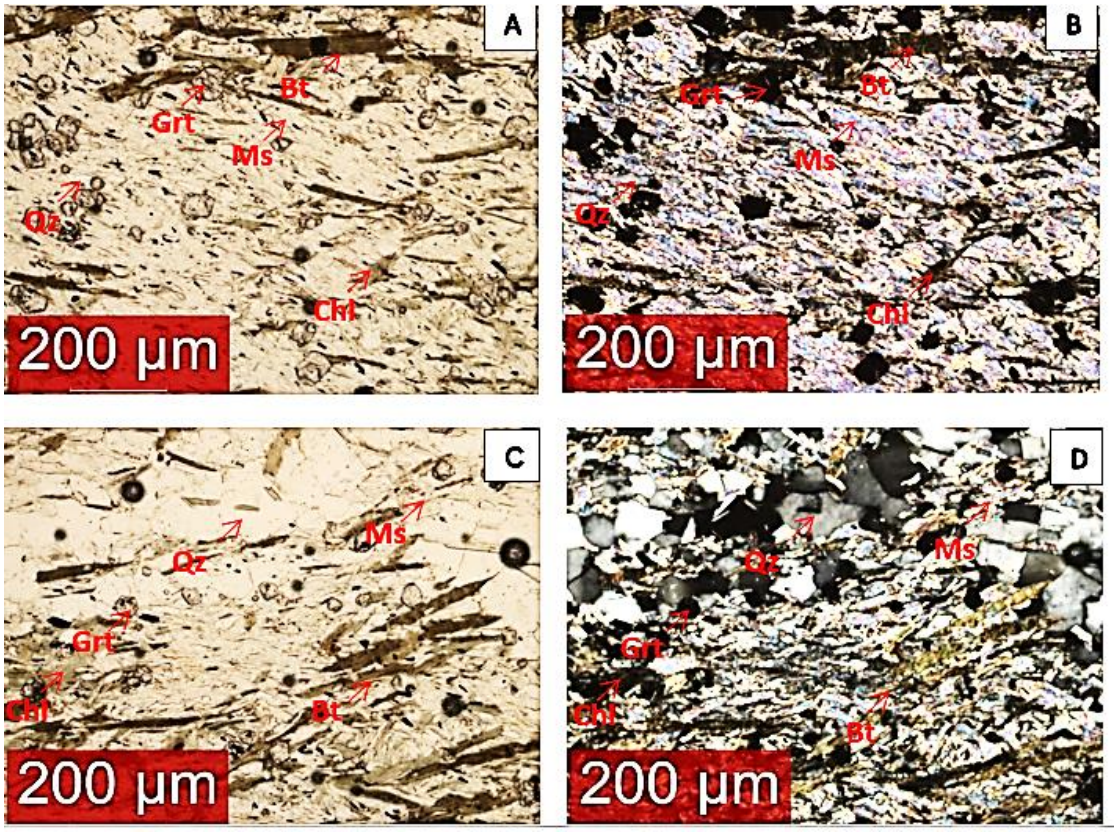

Figure 4. Photomicrographs of the main microstructural and textural features of PCM-441 sample. (A)-(B) Granolepidoblastic texture with very fine continue cleavage domain. PPL and XPL, respectively. (C)-(D) Lepidogranoblastic texture with polygonal aggregates, triple points and mineral growth in microlithons. PPL and XPL, respectively. PPL, plane polarized light; XPL, cross polarized light. Qz, quartz; Grt, garnet; Chl, chlorite; Bt, biotite; Ms, muscovite. Fuente: Autor(es).

4.2. Whole-rock chemistry

In conjunction with the petrographic analyses, three selected samples (PCM-417, PCM-420, and PCM-441) underwent bulk-rock chemistry analysis, providing valuable insights into the compositional variations within the metapelitic rocks of the studied region. Sample PCM-441 is distinguished by a notably lower SiO_2 content of 48.38%, contrasting sharply with the higher values observed in samples PCM-417 (68.32%) and PCM-420 (76.51%). This difference in silica content could signify variations in the protolith composition or reflect differing degrees of metamorphic alteration. Additionally, the Al_2O_3 content in sample PCM-441 is notably higher at 27.01%, compared to samples PCM-417 (14.49%) and PCM-420 (10.90%). This contrast may indicate differences in the mineral assemblages and metamorphic conditions experienced by the various samples. Examining other major components, TiO_2 exhibits variability ranging from 0.66% to 1.32%, FeO from 4.27% to 8.73%, MnO from 0.42% to 1.17%, MgO from 1.22% to 3.17%, CaO ranging between 0.63% and 1.41%, Na_2O varying from 1.51% to 3.07%, and K_2O ranging from 1.78% to 7.04%.

These fluctuations in major oxides suggest distinct mineralogical compositions and potential metamorphic histories for each sample. Moreover, the P_2O_5 content fluctuates between 0.04% and 0.24%, contributing to the overall chemical heterogeneity observed in the analyzed samples. The detailed whole-rock chemistry data obtained through WDXRF analysis is summarized in Table 1, providing a comprehensive view of the elemental composition of each sample. This information serves as a crucial foundation for further interpretations regarding the geological and metamorphic complexities of the Silgará Formation in the southwestern Santander Massif (Colombia).

Table 1. Whole-rock chemistry of metapelitic rocks of the Silgará Formation. Fuente: Autor(es).

Sample No.	SiO_2	Al_2O_3	TiO_2	FeO	MnO	MgO	CaO	Na_2O	K_2O	P_2O_5
PCM-417	68.32	14.49	0.66	8.73	1.17	1.42	1.22	3.07	1.70	0.04
PCM-420	76.51	10.90	0.72	4.27	0.42	1.50	1.41	2.45	1.78	0.24
PCM-441	48.38	27.01	1.32	8.60	1.10	3.17	0.63	1.51	7.04	0.15

Delgado and Suárez [49] suggest that the metapelitic rocks within the Silgará Formation have originated from sedimentary protoliths, primarily characterized by argillaceous rocks, as elucidated by De La Roche [50]. However, a more nuanced understanding emerges when considering the classification proposed by Herron [51]. In accordance with Herron's diagram, the sedimentary protoliths can be delineated as greywackes in the case of PCM-417 and as Fe-rich shales for PCM-420 and PCM-441. Delgado and Suárez [49] further utilized the AFM diagram devised by Thompson [52], a valuable tool in the analysis of metapelitic rocks within the MnNCKFMASH system. This diagram allows for the projection from phases in excess, such as quartz, muscovite, and H2O, to discern the relative aluminum content of the analyzed samples. As illustrated in Figure 5, the metapelitic rocks in focus exhibit a spectrum of aluminum content, with PCM-441 identified as relatively Al-rich shales, PCM-420 as poor-Al shales, and PCM-417 as very poor-Al shales. These deductions shed light on the diverse sedimentary protoliths and mineralogical compositions present within the Silgará Formation. The identification of greywackes and Fe-rich shales indicates a range of precursor materials, suggesting varied depositional environments or alteration processes. Additionally, the characterization of Al-rich, poor-Al, and very poor-Al shales provides crucial insights into the metamorphic history and subsequent mineral transformations experienced by these rocks. The chemical composition of garnet, as summarized in Figure 5, further complements these deductions, offering a comprehensive understanding of the metapelitic rocks' evolution within the MnNCKFMASH system.

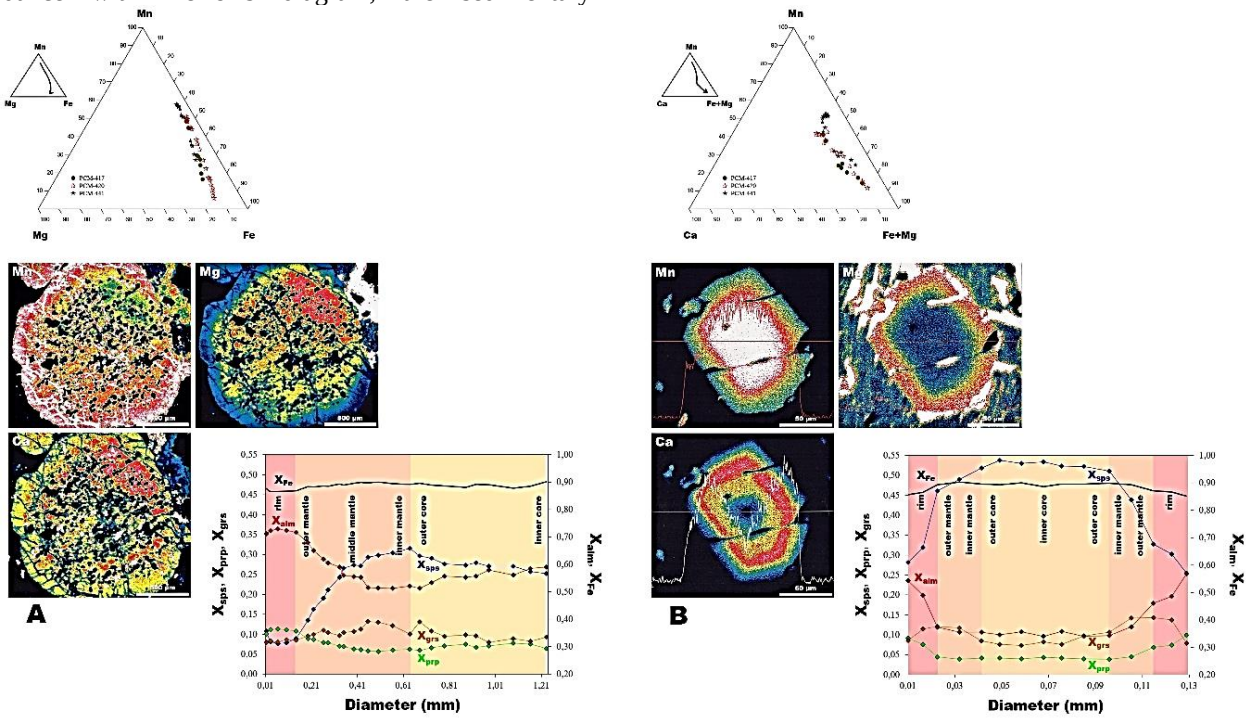

Figure 5. X-ray compositional maps and quantitative spot analysis of garnet in samples (A) PCM-420 and (B) PCM-441. Fuente: Autor(es).

4.3. Mineral chemistry

Garnet from the garnet zone exhibit a distinctive almandine-rich composition, with X_{alm} values ranging from 0.36 to 0.72. Additionally, minor constituents include spessartine (X_{sps} = 0.07-0.52), pyrope (X_{prp} = 0.04-0.12), and grossular (X_{grs} = 0.08-0.10). These compositional variations not only provide a unique fingerprint for the garnet samples but also offer valuable insights into the prevailing metamorphic conditions within the studied region. A noteworthy feature of the garnet crystals is the presence of typical growth zoning patterns,

indicative of distinct stages of crystallization and mineral growth. However, a compelling exception is observed in the sample from the sillimanite zone, where a diffusion-dominated zoning profile is identified, as reported by Ríos *et al*. [38]. This exceptional zoning pattern suggests a specialized metamorphic history for this particular sample, possibly involving rapid changes in pressure and temperature conditions during its formation. Importantly, the absence of a significant increase in manganese (Mn) at the garnet rims is a notable observation. This lack of pronounced late-stage resorption or cation exchange in the garnet structure indicates relative stability and equilibrium in the metamorphic environment. The preservation of garnet zoning patterns and the absence of major elemental alterations further contribute to our understanding of the metamorphic processes experienced by these rocks. Table 2 provides representative analyses of the garnet specimens, offering a detailed breakdown of their elemental composition. These mineral chemistry data serve as a critical foundation for unraveling the intricate metamorphic history of the Silgará Formation, providing researchers with key parameters to assess peak metamorphic conditions and gain insights into the dynamic geological processes that shaped these metapelitic rocks.

Table 2. Representative chemical compositions of garnet from metapelitic rocks in the garnet zone of the Silgará Formation. Fuente: Autor(es).

Metamorphic zone	Grt	Grt	Grt	Grt	Grt	Grt
Sample No.	PCM-417	PCM-417	PCM-420	PCM-420	PCM-441	PCM-441
Mineral	Grt	Grt	Grt	Grt	Grt	Grt
Weight %	rim	core	rim	core	rim	core
SiO_2	37.37	37.62	36.76	36.50	36.39	36.50
TiO_2	0.06	0.02	0.00	0.02	0.02	0.05
Al_2O_3	20.89	20.63	20.25	19.78	20.64	20.29
FeO*	32.39	31.19	31.22	26.86	25.42	16.63
MnO	3.17	4.90	4.68	10.97	12.28	23.43
MgO	3.05	2.66	2.47	1.59	2.26	1.09
CaO	3.27	3.42	2.72	3.19	2.95	2.84
Na_2O	0.03	0.04	0.01	0.04	0.00	0.04
K_2O	0.05	0.03	0.05	0.00	0.06	0.03
Cr_2O_3	0.00	0.02	0.02	0.00	0.00	0.00
Total	100.28	100.53	98.18	98.95	100.01	100.89
Cations per	12 O	12 O	12 O	12 O	12 O	12 O
Si	2.998	3.017	3.021	3.010	2.961	2.973
Ti	0.003	0.001	0.000	0.001	0.001	0.003
Al	1.975	1.950	1.961	1.922	1.979	1.947
Fe^{3+}	0.021	0.014	0.000	0.056	0.096	0.101
Fe^{2+}	2.152	2.078	2.146	1.796	1.633	1.031
Mn	0.215	0.333	0.326	0.766	0.846	1.616
Mg	0.365	0.318	0.303	0.195	0.275	0.132
Ca	0.281	0.293	0.239	0.282	0.257	0.247
Na	0.011	0.013	0.003	0.013	0.001	0.013
K	0.010	0.007	0.011	0.000	0.012	0.007
Cr	0.000	0.001	0.001	0.000	0.000	0.000
Total	8.031	8.025	8.012	8.041	8.061	8.070
*Total Fe as	$FeO+Fe_2O_3$					
X_{alm}	0.72	0.69	0.71	0.59	0.56	0.36
X_{sps}	0.07	0.11	0.11	0.25	0.27	0.52
X_{prp}	0.12	0.10	0.10	0.06	0.09	0.04
X_{grs}	0.09	0.10	0.08	0.09	0.08	0.08

The X_{Fe} ratio of biotite ranges from 0.43 to 0.72, indicative of variations in iron content. Al^{IV} exhibits variability between 2.454 and 2.988, while Al^{VI} ranges from 0.513 to 1.300 a.p.f.u., suggesting a slight solid solution trend toward dioctahedral micas. Titanium (Ti) content spans from 0.140 to 1.300 a.p.f.u. These compositional fluctuations underscore the diverse nature of biotite in the garnet zone. Muscovite displays a silicon (Si) content fluctuating between 6.092 and 6.312 a.p.f.u. Additionally, the celadonite content (X_{Si} = (Si/2)-3) varies from 0.05 to 0.16, while the Na/(Na+K) ratio ranges from 0.02 to 0.12. These variations in muscovite composition provide insights into the mineralogical heterogeneity within the garnet zone. In plagioclase, the anorthite content (X_{An}) ranges from 0.00 to 0.18, highlighting the range of calcium-aluminum feldspar compositions. Conversely, potassium feldspar shows lower values, with X_{An} ranging between 0.00 and 0.02. Table 3 presents representative analyses of biotite, muscovite, and feldspar in the garnet zone. The observed variations in elemental composition provide crucial data for understanding the mineralogical complexities and metamorphic conditions of the Silgará Formation. These results contribute valuable constraints for thermodynamic modeling and pseudosection construction, enhancing our interpretation of the metamorphic history in this geological context.

Table 3. Representative chemical compositions of biotite, muscovite and feldspar (plagioclase and potassium feldspar) from pelitic rocks of the Silgará Formation. Fuente: Autor(es).

Metamorphic zone	Grt	Grt	Grt	Grt	Grt	Grt	Grt	Grt	Grt
Sample No.	PCM-441	PCM-417	PCM-441	PCM-417	PCM-420	PCM-441	PCM-417	PCM-420	PCM-441
Mineral	Bt	Ms	Ms	Pl	Pl	Pl	Kfls	Kfls	Kfls
Weight %	core	core	n(Grt)	core	rim	core	core		core
SiO_2	34.20	46.02	44.54	68.26	66.94	62.66	64.39	61.48	64.20
TiO_2	11.91	0.33	0.32	0.05	0.00	0.00	0.00	0.00	0.00
Al_2O_3	24.84	30.55	32.39	20.12	20.18	22.82	19.10	23.60	18.29
FeO*	10.24	4.94	4.76	0.14	0.13	0.09	0.18	0.85	0.51
MnO	2.64	0.04	0.44	0.03	0.01	0.02	0.04	0.02	0.05
MgO	2.28	1.60	1.41	0.03	0.00	0.00	0.00	0.19	0.20
CaO	0.01	0.01	0.12	0.09	0.75	3.85	0.17	0.11	0.00
Na_2O	0.48	0.15	0.91	10.97	10.84	9.49	3.73	7.00	0.20
K_2O	8.14	11.21	10.26	0.16	0.12	0.43	10.62	4.59	18.53
Cr_2O_3	0.04	0.01	0.01	0.02	0.03	0.00	0.00	0.01	0.00
Total	94.78	94.86	95.17	99.87	99.00	99.36	98.23	97.85	101.99
Cations per	22 O	22 O	22 O	8 O	8 O	8 O	8 O	8 O	8 O
Si	5.012	6.312	6.092	2.981	2.802	2.795	2.973	2.802	2.960
Ti	1.313	0.034	0.033	0.002	0.000	0.000	0.000	0.000	0.000
Al	4.289	4.938	5.221	1.035	1.268	1.199	1.039	1.268	0.994
Fe^{3+}	0.000	0.000	0.000	0.000	0.032	0.000	0.000	0.032	0.000
Fe^{2+}	1.255	0.567	0.545	0.005	0.000	0.003	0.007	0.000	0.020
Mn	0.328	0.005	0.051	0.001	0.001	0.001	0.002	0.001	0.002
Mg	0.498	0.327	0.288	0.002	0.013	0.000	0.000	0.013	0.014
Ca	0.001	0.001	0.017	0.004	0.005	0.184	0.008	0.005	0.000
Na	0.136	0.040	0.240	0.929	0.618	0.821	0.334	0.618	0.018
K	1.521	1.961	1.791	0.009	0.267	0.024	0.625	0.267	1.090
Cr	0.005	0.001	0.002	0.001	0.000	0.000	0.000	0.000	0.000
Total	14.358	14.185	14.279	4.968	5.007	5.028	4.988	5.007	5.097
*Total Fe as									
X_{Fe}	0.72								
X_{Si}		0.16	0.05						
Na/(Na+K)		0.02	0.12						
X_{An}				0.00	0.01	0.18	0.02	0.01	0.00

Ilmenite displays a titanium (Ti) content ranging from 0.901 to 1.172 Ti a.p.f.u., with manganese (Mn) ranging from 0.009 to 0.042 Mn a.p.f.u. and iron (Fe) from 0.631 to 1.059 Fe a.p.f.u. Rutile, on the other hand, exhibits 1.933 Ti a.p.f.u., 0.001 Mn a.p.f.u., and 0.023 Fe a.p.f.u. Finally, magnetite demonstrates variability with 0.000 to 0.002 Ti a.p.f.u., 0.004 to 0.014 Mn a.p.f.u., and 2.969 to 3.988 Fe a.p.f.u. These distinct compositions provide essential information about the mineralogical diversity and potential metamorphic conditions within the studied rocks. Chlorite's X_{Mg} ranges from 0.33 to 0.56, illustrating variations in magnesium content. It also contains 0.157 to 0.331 Mn a.p.f.u. These values contribute to our understanding of the compositional

range of chlorite and its significance in the metamorphic evolution of the rocks. Epidote contains minor amounts of manganese (Mn) within the range of 0.117 to 0.217, adding to the overall complexity of its composition. The $Fe^{3+}/(Fe^{3+}+Al)$ ratio in epidote varies from 0.33 to 0.48, providing insights into the oxidation state and the role of aluminum in the mineral. Table 4 presents representative analyses of oxides, chlorite, and epidote, offering a detailed breakdown of their elemental compositions. These results contribute valuable information for discerning the mineralogical intricacies and metamorphic conditions within the Silgará Formation. The diverse compositions of these minerals are crucial indicators of the geological processes and alterations that have shaped the studied rocks.

Table 4. Representative chemical compositions of oxides, chlorite and epidote from pelitic rocks of the Silgará Formation. Fuente: Autor(es).

Metamorphic zone	Grt	Grt	Grt	Grt	Grt	Grt	Grt	Grt	Grt	Grt	Grt
Sample No.	PCM-417	PCM-417	PCM-420	PCM-417	PCM-420	PCM-417	PCM-420	PCM-441	PCM-417	PCM-420	PCM-441
Mineral	Rut	Ilm	Ilm	Mgt	Mgt	Chl	Chl	Chl	Ep	Ep	Ep
Weight %	core	core	crack	core	inc.	rim	rim	core	rim	crack	core
SiO_2	1.14	0.41	0.22	0.08	0.02	24.88	24.71	26.13	24.88	32.54	26.13
TiO_2	92.07	44.28	62.44	0.06	0.01	0.11	0.07	0.09	0.11	0.20	0.09
Al_2O_3	0.31	0.79	0.07	0.04	0.02	20.29	18.85	21.09	20.29	19.42	21.09
FeO*	0.99	46.79	30.21	92.29	89.99	26.23	31.65	23.18	26.23	13.47	23.18
MnO	0.03	1.82	0.41	0.44	0.09	1.17	1.73	0.89	1.17	0.74	0.89
MgO	0.16	0.71	0.01	0.00	0.02	12.86	8.72	16.62	12.86	0.41	16.62
CaO	0.71	0.19	0.04	0.00	0.00	0.04	0.03	0.05	0.04	20.01	0.05
Na_2O	0.03	0.03	0.00	0.09	0.01	0.00	0.01	0.00	0.00	0.01	0.00
K_2O	0.06	0.06	0.04	0.03	0.02	0.09	0.06	0.09	0.09	0.05	0.09
Cr_2O_3	0.05	0.03	0.01	0.01	0.00	0.01	0.01	0.00	0.01	0.02	0.00
Total	95.55	95.11	93.45	93.04	90.18	85.68	85.84	88.13	85.68	86.87	88.13
Cations per	2 O	3 O	3 O	4 O	4 O	28 O	28 O	28 O	25 O	25 O	25 O
Si	0.032	0.011	0.005	0.003	0.001	5.442	5.586	5.432	5.442	6.084	5.432
Ti	1.933	0.901	1.172	0.002	0.000	0.018	0.012	0.013	0.018	0.028	0.013
Al	0.010	0.025	0.002	0.002	0.001	5.231	5.022	5.167	5.231	4.279	5.167
Fe^{3+}	0.000	0.000	0.000	0.000	0.000	0.000	0.000	0.000	4.798	2.106	4.029
Fe^{2+}	0.023	1.059	0.631	2.969	3.988	4.798	5.982	4.029	0.000	0.000	0.000
Mn	0.001	0.042	0.009	0.014	0.004	0.217	0.331	0.157	0.217	0.117	0.157
Mg	0.007	0.029	0.000	0.000	0.002	4.194	2.939	5.151	4.194	0.114	5.151
Ca	0.021	0.006	0.001	0.000	0.000	0.009	0.007	0.010	0.009	4.008	0.010
Na	0.002	0.002	0.000	0.007	0.001	0.000	0.004	0.000	0.000	0.004	0.000
K	0.002	0.002	0.001	0.001	0.001	0.025	0.017	0.023	0.025	0.012	0.023
Cr	0.001	0.001	0.000	0.000	0.000	0.002	0.002	0.000	0.002	0.003	0.000
Total	2.031	2.077	1.822	2.998	3.999	19.936	19.902	19.982	19.936	16.755	19.982
*Total Fe as											
X_{Mg}						0.47	0.33	0.56			
$Fe^{3+}/(Fe^{3+}+Al)$									0.48	0.33	0.44

4.4. PT conditions

Understanding the peak metamorphic conditions, often expressed as temperature and pressure, is crucial for unraveling the geological history of a rock formation. In this study, investigating PT conditions is of paramount importance as it provides key insights into the thermal and tectonic evolution of the Silgará Formation in the southwestern Santander Massif, Colombia. The utilization of advanced methodologies such as Gibbs's free energy minimization, geothermobarometry, and pseudosections plays a pivotal role in this inquiry. These sophisticated techniques enable a comprehensive examination of mineral assemblages, allowing researchers to deduce the prevailing thermodynamic conditions during the formation of metamorphic rocks. By integrating thermodynamic principles, geothermobarometric calculations, and pseudosection modeling, this study aims to delineate the intricate metamorphic processes, contributing not only to the understanding of the Silgará Formation but also showcasing the significance of employing cutting-edge methods in deciphering the geological complexities of metamorphic terrains.

4.4.1. Minimization of the Gibbs´s free energy

The application of minimization of Gibbs's free energy (Figure 6), as demonstrated through the THERMOCALC methodology [53], has yielded valuable insights into the equilibrium conditions of mineral phases within the garnet zone of the Silgará Formation. Analyzing the results obtained from bulk-rock chemistry at constant pressures, distinct temperature ranges have been identified for each sample, shedding light on the intricate thermodynamic stability of mineral assemblages.

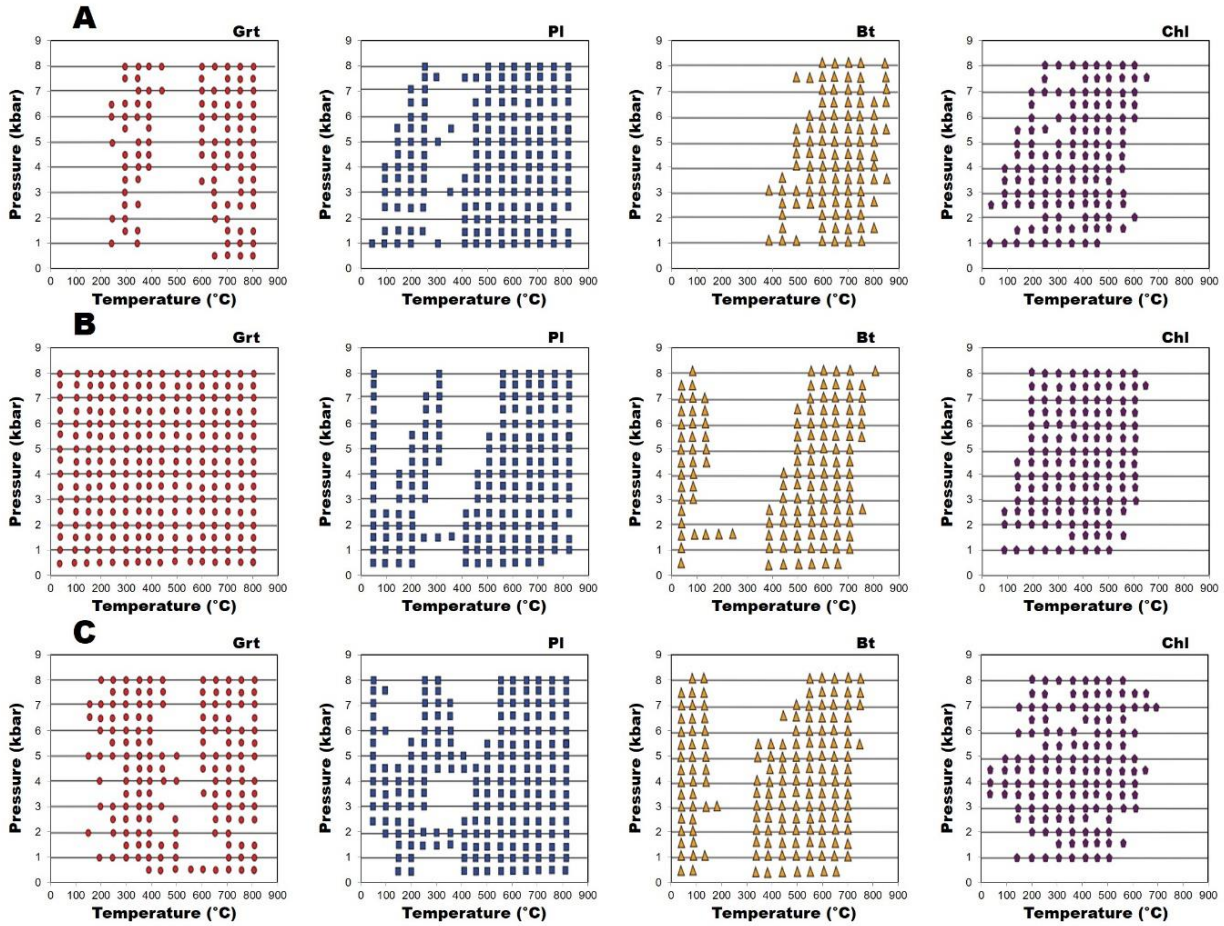

Figure 6. Ranges of equilibrium for the mineral phases sensible to pressure and temperature changes for the (A) PCM-417, (B) PCM-420, and (C) PCM-441 samples. Grt, garnet; Pl, plagioclase; Bt, biotite; Chl, chlorite. Symbols represent the invariant points where a stable equilibrium for each mineral phase occurs. Fuente: Autor(es).

Results are given in the following temperature ranges: PCM-417 sample (Figure 6A) shows totally stable chlorite, muscovite and quartz across a broad temperature spectrum. In contrast, minerals such as garnet (250-450 °C and 600-800 °C), plagioclase (100-250 °C and 450-850 °C) and biotite (300-800 °C) biotite exhibit varied equilibrium conditions at different pressures and temperatures, providing a nuanced understanding of their metamorphic evolution. PCM-420 sample (Figure 6B) reveals that garnet, quartz and muscovite remain consistently stable, showcasing their equilibrium across distinct temperature intervals. Conversely, plagioclase (50-300 °C and 400-800 °C), biotite (50-150 °C and 400-750 °C) and chlorite (200-600 °C) display varying equilibrium conditions at multiple pressures and temperatures, contributing to a comprehensive characterization of the metamorphic processes. PCM-441 sample (Figure 6C) shows totally stable muscovite and quartz over specific temperature ranges. Meanwhile, plagioclase (50-200 °C and 500-800 °C), garnet (200-500 °C and 600-800 °C), biotite (50-150°C and 350-700 °C) and chlorite (200-600 °C) showcase diverse equilibrium conditions at different pressures and temperatures, providing critical data for understanding the complex metamorphic history. Overall, these results enable to deduce the temperature-pressure conditions under which specific mineral phases were stable, offering a comprehensive framework for reconstructing the metamorphic evolution of the Silgará Formation in the southwestern Santander Massif, Colombia.

4.4.2. Geothermobarometry

Geothermobarometry was employed to assess the PT conditions in the garnet zone of the Silgará Formation within the SWSM. Using the GTB software, PT conditions were determined for the analyzed PCM-441 sample, and the results are illustrated in Figure 7. The calculations involved the garnet-biotite (GB) Fe-Mg exchange thermometer, as well as the garnet-biotite-muscovite-plagioclase (GBMP) and garnet- Al_2SiO_5-quartz-plagioclase (GASP) barometers, considering the calibrations developed by several authors [13,54-60], with a focus on selecting those in best agreement with the expected PT conditions within the equilibrium stability fields for each mineral. In the garnet zone (PCM-441 sample), pressure conditions are in the range of 3.0-5.9 kbar, limited by the calibrations of Powell and Holland [13] as the upper limit and Ghent and Stout-Fe [56] as the lower limit,

whereas temperature conditions are in the range of 400-500 °C, limited by the calibrations of Ferry and Spear [54] as the left-side limit and Kleeman and Reinhardt [60] as the right-side limit. The middle point for the garnet zone is at c. 4.2 kbar and 450 °C. PT conditions for the garnet zone (PCM-441 sample) of the Silgará Formation at the SWSM, using the software GTB are in the range of 3.0-5.9 kbar and 400-500 ºC. These geothermobarometric results, supported by robust calibrations and visualizations, contribute significantly to characterizing the metamorphic history in this geological context.

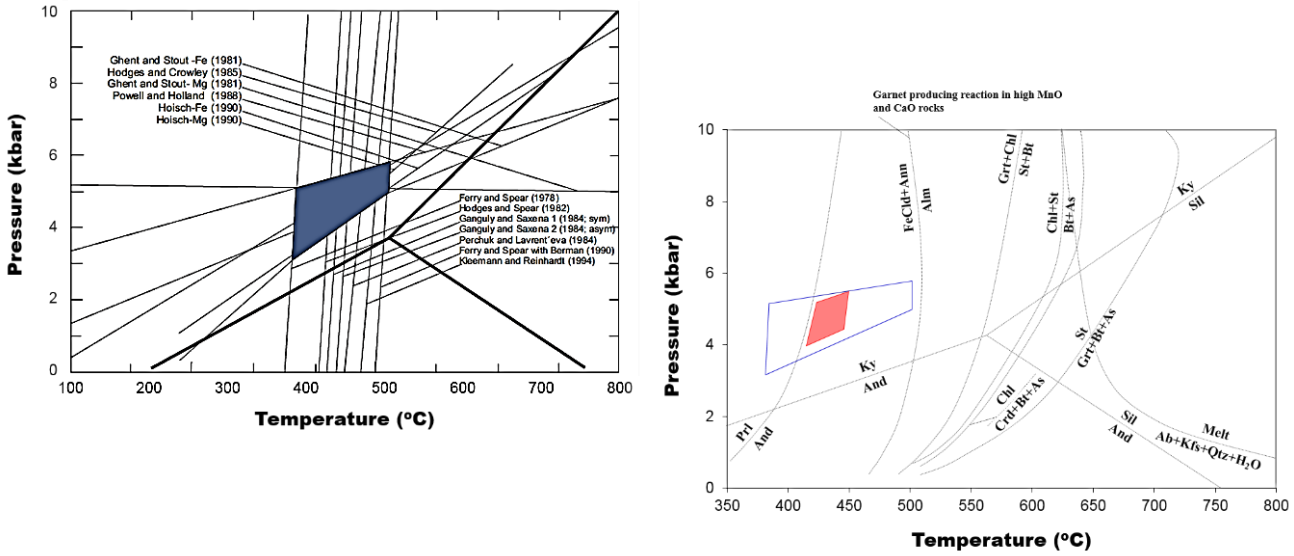

Figure 7. Geothermobarometry data plotted using the GTB program by Spear and Kohn [15], showing the PT ranges for the garnet metamorphic zone of the Silgará Formation at the SWSM. PT conditions are indicated by the blue box. GB thermometer calibrations (subvertical lines); GPBM barometer calibrations (subhorizontal lines). Fuente: Autor(es).

4.4.3. Pseudosections

Due to scarce texturally recognizable mineral reactions in metapelitic rocks, other methods for deciphering PT paths were explored. The Gibbs program [16] was discarded in view of the unknown PT range of the mineral assemblages. A pseudosection (equilibrium phase diagram) is a type of phase diagram that illustrates the fields of stability of different mineral assemblage equilibrium for a single bulk-rock composition. Pseudosections are one of the most useful tools to interpret the formation conditions of metamorphic rocks because they are simpler to read than their full grid equivalents, they can show the boundaries of fields of higher thermodynamic variance and they can be used to portray other information [61]. Therefore, they are generally simpler and much easier to interpret than standard phase diagrams that show many reactions. Pseudosections for a fixed rock composition offer a more rigorous treatment and have been applied, for example, to metapelitic rocks with programs such as THERMOCALC [62-65] and Domino [66]. In order to reduce uncertainties in the whole-rock composition and amount of fluid, samples with carbonate were discarded. The Silgará Formation is mainly composed of pelitic rocks, which can be characterized in the KFMASH systems with the following components: SiO_2, Al_2O_3, FeO, MgO, K_2O and H_2O, along with minor components, such as TiO_2, MnO, Na_2O and CaO. These rocks are good indicators of metamorphism due to their sensibility to pressure and temperature changes [48]. The chemical systems can be represented by phase diagrams, which show what mineral phase or mineral assemblage is more stable in function of pressure and temperature conditions [67]. The determination of the chemical system to obtain the pseudosections based on the previously defined mineral assemblages and mineral composition, e.g., considering the chemical formulae of garnet and biotite, the simplified KFMASH (K_2O-FeO-MgO-Al_2O_3-SiO_2-H_2O) system was considered for these mineral phases, which was also applied to all mineral phases. However, this chemical system does not consider the MnO, Na_2O and CaO components for the prediction of the mineral stability in the pseudosection. Therefore, we consider the MnNCKFMASH (MnO-Na_2O-CaO-K_2O-FeO-MgO-Al_2O_3-SiO_2-H_2O) system, which consider the effect of MnO and CaO, determining the equilibrium state of garnet and zoisite (precursor phase of garnet), and Na_2O, defining the stability of plagioclase, paragonite and clinozoisite [1]. In this study, the pseudosections (Figure 8), which show the PT stability fields of mineral assemblages, were constructed using the THERIAK/DOMINO software of De Capitani and Petrakakis [68]. The Domino program calculates equilibrium assemblage phase diagrams using Gibbs free energy minimization, and the used thermodynamic data were taken mostly from the internally consistent database supplied with the program. PT conditions estimated for the mineral assemblages of each sample from the garnet zones of the Silgará Formation at the SWSM that means, showing the

equilibrium field of PT reached by the samples during the metamorphic event according to the mineral assemblages. Figure 8A shows the pseudosection for PCM-417 sample in the MnNCKFMASH system, which reveals that the mineral assemblage of the rock coexists in the stability field of garnet + biotite + muscovite + plagioclase + chlorite + quartz, establishing ranges of pressure of 0-8 kbar and temperature of 310-500 °C. Figure 8B shows the pseudosection for PCM-420 sample in the MnNCKFMASH system, which reveals that the mineral assemblage of the rock coexists in the stability field of garnet + biotite + muscovite + plagioclase + chlorite + quartz, establishing ranges of pressure of 0-9.5 kbar and temperature of 380-520 °C. Figure 8C shows the pseudosection for PCM-441 sample in the MnNCKFMASH system, which reveals that the mineral assemblage of the rock coexists in the stability field of garnet + biotite + muscovite + plagioclase + chlorite + quartz, establishing ranges of pressure of 0-9 kbar and temperature of 350-550 °C. These data agree with the equilibrium of each mineral phase given by the minimization of the Gibbs energy.

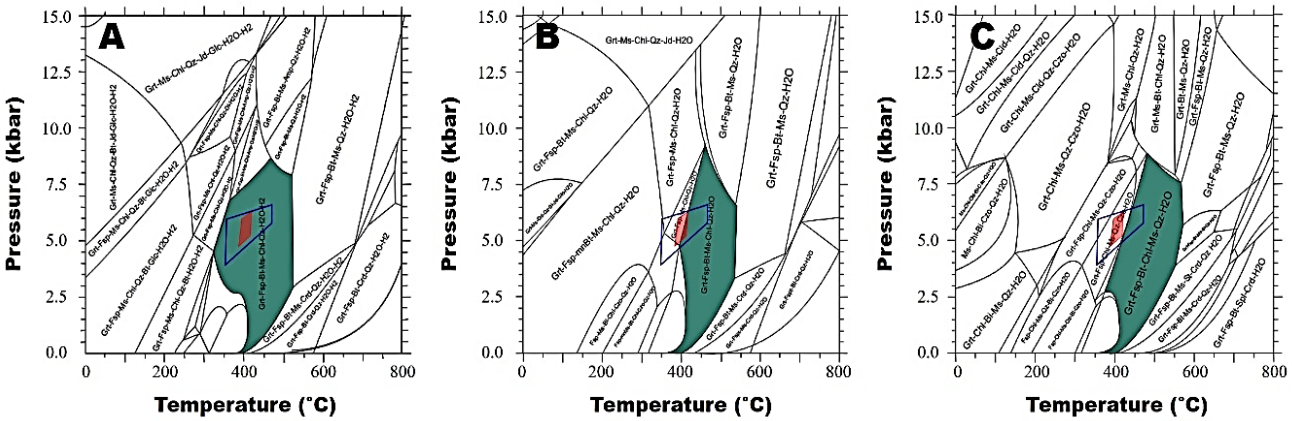

Figure 8. PT pseudosections in the MnNCKFMASH system with quartz and H_2O excess conditions calculated with THERIAK/DOMINO software of De Capitani and Petrakakis [68] for (A) PCM-417, (B) PCM-420, and (C) PCM-441 samples from the garnet zone of the Silgará Formation. The shadow areas represent the PT stability fields of mineral assemblages. Fuente: Autor(es).

The geothermobarometric data derived from this study, utilizing the GTB software, has unveiled a broader spectrum of PT conditions within the garnet zone of the Silgará Formation, ranging from 3.0 to 5.9 kbar and 400 to 500 °C. This extended range contrasts with the PT conditions (4.4-5.5 kbar and 495-518 °C) previously reported by Ríos *et al*. [38]. While our findings align with certain limits of the previous study, it's important to note that we meticulously selected calibrations for each thermometer and barometer, contributing to a nuanced understanding of the metamorphic conditions.

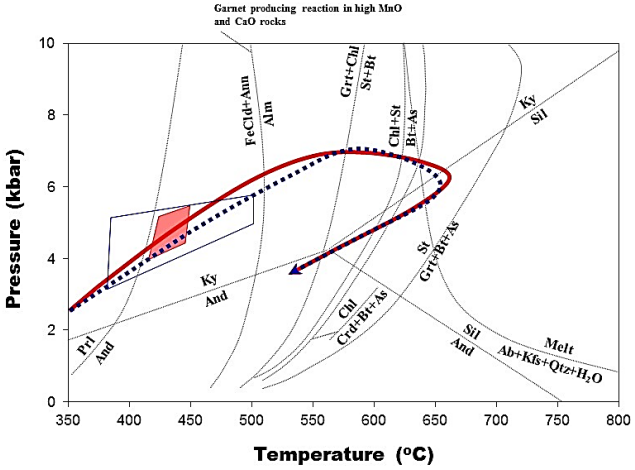

Figure 9. PT diagram, showing the overlapping of the geothermobarometric data obtained in this study using the software GTB (polygons of blue border) and those reported by Ríos *et al*. [38] (red polygons) for the garnet metamorphic zone of the Silgará Formation at the SWSM, the mineral reactions in the MnCKFMASH system of the petrogenetic grid (adapted and modified after Spear and Cheney [9] and Spear [69], and the clockwise PT paths proposed in this study (blue dotted arrow) and by Ríos *et al.* [38] (red arrow) and. Al_2SiO_5 triple point after Holdaway *et al*. [70]. Fuente: Autor(es).

A critical evaluation of our PT ranges against the petrogenetic grid proposed by Spear and Cheney [9] reveals a remarkable agreement between the observed PT conditions and the metamorphic equilibrium zones for each sample, as

depicted in Figure 9. Notably, the P_{peak} maximum coincides with the mineral assemblage garnet + potassium feldspar + biotite + muscovite + quartz in the presence of H_2O. This suggests the stabilization of this mineral assemblage at the T_{peak} maximum, providing valuable insights into the peak metamorphic conditions experienced by the Silgará Formation in the southwestern Santander Massif, Colombia. The refined geothermobarometric data presented here not only enriches our understanding of the Silgará Formation's metamorphic history but also highlights the importance of comprehensive calibration selections in achieving robust and accurate PT determinations.

The utilization of a PT pseudosection modeling approach proves to be a valuable tool for unraveling the intricate tectono-metamorphic evolution within the SWSM. This method hinges on garnet mineralogy, chosen for its sensitivity to variations in pressure-temperature (PT) conditions. Garnet stands out as an exceptional PT recorder during geological events due to its responsiveness to changes in the metamorphic environment. Moreover, the well-established solution model of garnet further enhances its utility in constructing accurate pseudosections. By leveraging garnet mineralogy in the pseudosection, profound insights into the thermal and tectonic history of the Silgará Formation can be gained. This modeling approach serves as a dynamic framework, allowing researchers to decipher the complex metamorphic processes that have shaped the geological evolution of the studied region.

5. Conclusions

Quantitative phase diagrams, known as PT pseudosections, were generated in the MnNCKFMASH system under quartz and H2O excess conditions using the THERIAK/DOMINO software. These pseudosections were constructed based on metapelitic rocks sampled from the garnet, staurolite, and sillimanite zones of the Silgará Formation in the SWSM. The modeling considered the equilibrium of mineral phases, coupled with geothermobarometry data specific to each metamorphic zone. The results point to pressure and temperature conditions for the stability fields within each pseudosection, ranging from 3.0 to 5.9 kbar and from 400 to 500 °C. Upon reevaluating the geothermobarometry data and examining the equilibrium of mineral phases, the findings unveil maximum pressure conditions (P_{peak}) within the staurolite zone and maximum temperature conditions (T_{peak}) within the sillimanite zone. This concurrence strongly supports the interpretation of a clockwise PT path for the Silgará Formation, aligning with the metamorphic evolution observed in the field. It is crucial to note that the appearance of specific mineral phases associated with each metamorphic zone is intricately linked to the bulk-rock composition and the prevailing PT conditions. While the initial assessment of metamorphic conditions is a valuable approximation, a more accurate determination can be achieved through the combination of equilibrium modeling and geothermobarometry of mineral phases. This integrated approach provides a robust framework for understanding the metamorphic history and the dynamic geological processes that shaped the Silgará Formation in the SWSM.

Acknowledgements. The authors gratefully acknowledge the Shimane University and Universidad Industrial de Santander for the use of research facilities. We thank to the Electron Probe Microanalysis Laboratory at Shimane University and the X-ray and Microscopy laboratories at Universidad Industrial de Santander and their professional staff for assistance with data acquisition. This study has benefited from these entities and their human resources. Authors also thank members of the Research Group in Basic and Applied Geology for their helpful discussions and constructive comments. We express thanks to anonymous reviewers for helpful comments and suggestions of this manuscript. We are most grateful to the above-named people and institutions for support.

References

[1] Tinkham, D.K., Zuluaga, C.A., Stowell, H.H. Metapelite phase equilibria modeling in MnNCKFMASH: the effect of variable Al_2O_3 and MgO/MgO+FeO on mineral stability. Min. Soc. Am.: Geol. Mater. Res. 3 (2001) 1-42.

[2] Jowhar, T.N. Computer Programs for PT History of Metamorphic Rocks using Pseudosection Int. J. Comput. Appl. 418 (2012) 18-25.

[3] Berman, R.G. Internally-consistent thermodynamic data for minerals in the system Na_2O-K_2O-CaO-MgO-FeO-Fe_2O_3-Al_2O_3-SiO_2-TiO_2-H_2O-CO_2. J. Petrol. 292 (1988) 445-522.

[4] Holland, T.J.B., Powell, R. An internally consistent thermodynamic dataset for phases of petrological interest. J. Metamorph. Geol. 163 (1998) 309-343.

[5] Holland, T.J.B., Powell, R. An improved and extended internally consistent thermodynamic dataset for phases of petrological interest, involving a new equation of state for solids. J. Metamorph. Geol. 293 (2011) 333-383.

[6] Horváth, P. PT pseudosections in KFMASH, KMnFMASH, NCKFMASH and NCKMnFMASH systems: a case study from garnet-staurolite mica schist from the Alpine metamorphic basement of the Pannonian Basin Hungary. Geol. Carpath. 582 (2007) 107-119.

[7] Pattison, D.R.M., Tracy, R.J. Phase equilibria and thermobarometry of metapelites, in: D.M. Kerrick (Eds.), Contact Metamorphism Reviews in Mineralogy 26, Mineralogical Society of America, Washington, DC (1991) 105-206.

[8] Droop, G.T.R., Harte, B. The effect of Mn on the phase relations of medium-grade pelites: constraints from natural assemblages on petrogenetic grid topology. J. Petrol. 36 (1995) 1549-1578.

[9] Spear, F.S., Cheney, J. A petrogenetic grid for pelitic schists in the system SiO_2–Al_2O_3–FeO–MgO–K_2O–H_2O. Contrib. Mineral. Petrol. 101 (1989) 149-164.

[10] 0Powell, R., Holland, T.J.B. Calculated mineral equilibria in the pelite system KFMASH K_2O-FeO-MgO-Al_2O_3-SiO_2-H_2O. Am. Mineral. 75 (1990) 367-380.

[11] Mahar, E.M., Baker, J.M., Powell, R., Holland, T.J.B., Howell, N. The effect of Mn on mineral stability in metapelites. Contrib. Mineral. Petrol. 99 (1997) 226-237.

[12] White, R.W., Powell, R., Holland, T.J.B. Calculation of partial melting equilibria in the system Na_2O-CaO-K_2O-FeO-MgO-Al_2O_3-SiO_2-H_2O NCKFMASH. J. Metamorph. Geol. 19 (2001) 139-153.

[13] Powell, R., Holland, T.J.B. An internally consistent dataset with uncertainties and correlations: 3. Applications to geobarometry, worked examples and a computer program. J. Metamorph. Geol. 6 (1988) 173-204.

[14] De Capitani, C. Gleichgewichts phasendiagramme: theorie und software. Eur. J. Mineral. 6 (1994) 48–72.

[15] Spear, F.S., Kohn, M.J. Program GTB: GeoThermoBarometry. Rensselaer Polytechnic Institute (2001). 30 March 2006. http://ees2.geo.rpi.edu/MetaPetaRen/GTB_Prog/GTB.html

[16] Spear, F.S., Peacock, S.M., Kohn, M.J., Florence, F.P., Menard, T. Computer programs for petrologic PTt path calculations. Am. Mineral. 76 (11-12) (1991) 2009-2012.

[17] Audemard, F.E., Audemard, F.A. Structure of the Mérida Andes, Venezuela: relations with the South America-Caribbean geodynamic interaction. Tectonophysics 345 (2002) 299-327.

[18] Jimenez, G., Speranza, F., Faccena, C., Bayona, G., Mora, A. Magnetic stratigraphy of the Bucaramanga alluvial fan: Evidence for a ≤ 3 mm/yr slip rate for the Bucaramanga - Santa Marta Fault, Colombia. J. South Am. Earth Sci. 57 (2015) 12-22.

[19] Ward, D.E., Goldsmith, R., Cruz, B.J., Jaramillo, C.L., Restrepo, H. Geología de los Cuadrángulos H-12, Bucaramanga y H-13, Pamplona, Departamento de Santander. U.S. Geological Survey e Ingeominas. Bol. Geol. XXI (1-3) (1973) 1-132.

[20] Mantilla, L.C., García, C.A., Valencia, V.A. Propuesta de escisión de la denominada "Formación Silgará" (Macizo de Santander, Colombia), a partir de edades U-Pb en circones detríticos. Bol. de Geol. 381 (2016) 33-50.

[21] Goldsmith, R., Marvin, R., Mehnert, H. Radiometric ages in the Santander Massif, eastern Cordillera, Colombian Andes. U.S. Geol. Surv. Prof. Pap. 750-D (1971) D41-D49.

[22] Banks, P., Vargas, R., Rodríguez, G.I., Shagam, R. Zircon U-Pb ages from orthogneiss, Pamplona, Colombia. VI Congreso Latinoamericano de Geología, Bogotá, Colombia, 9-12 October, 1985.

[23] Dörr, W., Grösser, J., Rodriguez, G., Kramm, U. Zircon U-Pb age of the Páramo Rico tonalite-granodiorite, Santander Massif Cordillera Oriental, Colombia and its geotectonic significance. J. South Am. Earth Sci. 82 (1995) 187-194.

[24] Restrepo-Pace, P. Late Precambrian to Early Mesozoic tectonic evolution of the Colombian Andes, based on new geochronological, geochemical and isotopic data. Ph.D. Thesis (Unpublished), University of Arizona (1995) 195 p.

[25] Ordoñez, J.C. Petrology and geochemistry of the granitoids at the Santander Massif, Eastern Cordillera, Colombian Andes. M.Sc. Thesis (Unpublished), Shimane University (2003) 150 p.

[26] Ordoñez, J.C., Mantilla, L.C. Significance of an early Cretaceous Rb-Sr age in the Pescadero Pluton, Santander Massif. Bol. de Geol. 2643 (2004) 115-126.

[27] Mantilla, L.C., García, C.A., Ríos, C.A., Castellanos, O.M., Valencia, V.A., Camacho, D. Geocronología U-Pb en circones detríticos de rocas metasedimenarias del Macizo de Santander, Cordillera Oriental Colombia: Implicaciones estratigráficas. XV Congreso Colombiano de Geología, Bucaramanga, Colombia, Agosto 31 - Septiembre 5, 2015.

[28] Mantilla, L.C., Bissig, T., Cottle, J.M., Hart, C. Remains of early Ordovician mantle-derived magmatism in the Santander Massif (Colombian Eastern Cordillera). J. South Am. Earth Sci. 38 (2012) 1-12.

[29] Schäfer, J., Grösser, J., Rodríguez, G. Proterozoic Formación Silgará, Cordillera Oriental, Colombia: metamorphism and geochemistry of amphibolites. Zbl. Geol. Palaeont. Teil I 3-6 (1998) 531-546.

[30] Pace, P.R., Ruiz, J., Gehrels, G., Cosca, M. Geochronology and Nd isotopic data of Grenville-age rocks in the Colombian Andes: New constraints for late Proterozoic-early Paleozoic Paleocontinental reconstruction of the Americas. Earth Planet. Sci. Lett. 150 (1997) 427-441.

[31] Ríos, C.A. Chemical compositions of the constituent minerals and PT conditions of the low-grade Silgará Formation metamorphic rocks in the Santander Massif, Eastern Cordillera, Colombian Andes. M.Sc. Thesis (Unpublished), Shimane University (1999) 207 p.

[32] Ríos, C.A. Occurrence, chemical composition and genetic significance of the biotite in the Silgará Formation metamorphic rocks, southwestern Santander Massif, Eastern Cordillera, Colombian Andes. Bol. de Geol. 2338 (2001) 41-49.

[33] Ríos, C.A. Cation substitutions governing the chemistry of amphibole in the Silgará Formation metabasites at the southwestern Santander Massif. Bol. de Geol. 272 (2005) 13-30.

[34] Castellanos, O.M. Chemical composition of the rock-forming minerals in the Silgará formation and PT conditions in the Mutiscua area, Santander Massif, Eastern Cordillera, Colombia. M.Sc. Thesis (Unpublished), Shimane University (2001) 146 p.

[35] Mantilla, L.C., Ordoñez, J., Cepeda, S., Ríos, C.A. Study of the paleofluids in the Silgará Formation and their relationship with deformation processes, Aratoca-Pescadero area southwestern Santander Massif. Bol. de Geol. 2338 (2001) 69-75.

[36] Mantilla, L.C., Ríos, C.A., Castellanos, O. Study of the rehydratation process of the Silgará Formation metamorphic rocks, from the compositional analysis of chlorite, southwestern Santander Massif. Bol. de Geol. 2439 (2002) 7-17.

[37] Mantilla, L.C., Ríos, C.A., Gélvez, J., Márquez, R., Ordoñez, J., Cepeda, S. New evidences on the presence of a shear band in the metapelitic sequence of the Silgará Formation, Aratoca-Pescadero area southwestern Santander Massif. Bol. de Geol. 2540 (2003) 81-89.

[38] García, C.A., Ríos, C.A., Takasu, A. Tectono-metamorphic evolution of the Silgará Formation metamorphic rocks in the southwestern Santander Massif, Colombian Andes. J. South Am. Earth Sci. 16 (2003) 133-154.

[39] Ríos, C.A., Castellanos, O.M., Takasu, A. A new interpretation for the garnet zoning in metapelitic rocks of the Silgará Formation, southwestern Santander Massif, Colombia. Earth Sci. Res. 12 (2008) 7-30.

[40] Ríos, C.A., Castellanos, O.M., Gómez, S.I., Avila, G. Petrogenesis of the metacarbonate and related rocks of the Silgará Formation, central Santander Massif, Colombian Andes: An overview of a "reaction calcic exoscarn". Earth Sci. Res. 12 (2008) 72-106.

[41] Cardona, A. Correlacoes entre fragmentos do embasamento Pre-Mesozoico da terminacao setentrional dos Andes Colombianos, com base em datos isotopicos e geocronologicos. M.Sc. Thesis (Unpublished), Universidade de Sao Paulo (2003) 149 p.

[42] Castellanos, O.M., Ríos, C.A., Takasu, A. Chemically sector-zoned garnets in the metapelitic rocks of the Silgará Formation in the central Santander Massif, Colombian Andes: occurrence and growth history. Bol. de Geol. 26 (2004) 91-98.

[43] Castellanos, O.M., Ríos, C.A., Takasu, A. A new approach on the tectonometamorphic mechanisms associated with P–T paths of the Barrovian-type Silgará Formation at the Central Santander Massif, Colombian Andes. Earth Sci. Res. 12 (2008) 125-155.

[44] Castellanos, O.M., Ríos, C.A., Takasu, A. X-ray color maps of the zoned garnets from Silgará Formation metamorphic rocks, Santander Massif, Eastern Cordillera Colombia. Earth Sci. Res. 14 (2010) 161-172.

[45] García, C.A., Ríos, C.A., Castellanos, O.M. Medium-pressure metamorphism in the central Santander Massif, Eastern Cordillera, Colombian Andes: constraints for a collision model. Bol. de Geol. 27 (2005) 43-68.

[46] Ward, D.E., Goldsmith, R., Jimeno, V., Cruz, B.J., Restrepo, H., Gómez, R. (1969). Mapa Geológico del Cuadrángulo H-12, Bucaramanga, Colombia. Ingeominas.

[47] Ward, D.E., Goldsmith, R., Cruz, B.J., Jaramillo, C.L., Vargas, L.R. (1970). Mapa Geológico del Cuadrángulo H-13, Pamplona, Colombia. Ingeominas.

[48] Melgarejo, J.C. Atlas de asociaciones minerales en lámina delgada, Volumen 1. Universidad de Barcelona, Fundació Folch Barcelona. Edicions Universitat Barcelona (2003) 1071 p.

[49] Delgado, P.G., Suárez, A.M. Reevaluación y reinterpretación de datos de termobarometría y equilibrio de fases minerales de la Formación Silgará empleando THERMOCALC y THERIAK DOMINO. Undergraduate Thesis (Unpublished), Universidad Industrial de Santander (2015) 85 p.

[50] De La Roche, H. Comportement géochimique différentiel de Na, K et Al dans les formations volcaniques et sédimentaires: un guide pour l'étude des formations métamorphiques et plutoniques. C. R. Acad. Sci. Paris Sér. 267 (1968) 39–42.

[51] Herron, M. Geochemical classification of terrigenous sands and shales from core or log data. J. Sediment. Petrol. 58 (1988) 820–829.

[52] Thompson Jr, J. The graphical analyses of mineral assemblages in pelitic schists. Am. Mineral. 42 (1957) 842–858.

[53] Powell, R., Holland, T.J.B. Optimal geothermometry and geobarometry. Am. Mineral. 79 (1994) 120–133.
[54] Ferry, J.M., Spear, F.S. Experimental calibration of the partitioning of Fe and Mg between biotite and garnet. Contrib. Mineral. Petrol. 66 (1978) 113-117.
[55] Perchuk, L.L., Lavrent'eva, W. Experimental investigation of exchange equilibria in the system cordierite-garnet-biotite. In Kinetics and equilibrium in mineral reactions (Saxena, S.K. editor). Springer (1983) 199-239. New York.
[56] Ghent, E.D., Stout, M.Z. Geobarometry and geothermometry of plagioclase-biotite-garnet-muscovite assemblages. Contrib. Mineral. Petrol. 76 (1981) 92-97.
[57] Hodges, K.V., Spear, F.S. Geothermometry, geobarometry and the Al2SiO5 triple point at Mt. Moosilauke, New Hampshire. Am. Mineral. 67 (1982) 1118-1134.
[58] Ganguly, J., Saxena, S.K. Mixing properties of aluminosilicate garnets: Constraints from natural and experimental data, and applications to geothermo-barometry. Am. Mineral. 69 (1984) 88-97.
[59] Hoisch, T.D. Empirical calibration of six geobarometers for the mineral assemblage quartz + muscovite + biotite + plagioclase + garnet. Contrib. Mineral. Petrol. 104 (1990) 225-234.
[60] Kleemann, U., Reinhardt, J. Garnet-biotite thermometry revisited: The effect of AlVI and Ti in biotite. Eur. J. Mineral. 6 (1994) 925–941.
[61] Stüwe, K. Some calculated thermodynamic pseudosections from the Plattengneis and other rocks from the Koralm crystallime complex, Eastern Alps. Mitt. Naturwiss Ver. Steimark 124 (1994) 29-39.
[62] Will, T., Okrusch, M., Schmadicke, E., Chen, G. Phase relations in the greenschist–blueschist–amphibolite–eclogite facies in the system Na_2O–CaO–FeO–MgO–Al_2O_3–SiO_2–H_2O (NCFMASH), with application to metamorphic rocks from Samos, Greece. Contrib. Mineral. Petrol. 132 (1998) 85–102.
[63] Carson, C.J., Powell, R., Clarke, G.L. Calculated mineral equilibria for eclogites in CaO–Na_2O–FeO–MgO–Al_2O_3–SiO_2–H_2O: application to the Poue´bo Terrane, Pam Peninsula, New Caledonia. J. Metamorph. Geol. 17 (1999) 9–24.
[64] Carson, C.J., Clarke, G.L., Powell, R. Hydration of eclogite, Pam Peninsula, New Caledonia. J. Metamorph. Geol. 18 (2000) 79–90.
[65] Arnold, J., Powell, R., Sandiford, M. Amphibolites with staurolite and other aluminous minerals: calculated mineral equilibria in NCFMASH. J. Metamorph. Geol. 18 (2000) 23-40.
[66] Meyre, C., De Capitani, C., Partzsch, J.H. A ternary solid solution model for omphacite and its application to geothermobarometry of eclogites from the Middle Adula nappe Central Alps, Switzerland. J. Metamorph. Geol. 15 (1997) 687–700.
[67] Best, M. Igneous and metamorphic petrology. Blackwell Publishing (2008) 717 p. Nueva Jersey.
[68] De Capitani, C., Petrakakis, K. The computation of equilibrium assemblage diagrams with Theriak/Domino software. Am. Mineral. 95 (2010) 1006-1016.
[69] Spear, F.S. Metamorphic Phase Equilibria and Pressure-Temperature-Time Paths. Mineralogical Society of America (1993) 799 p. Chantilly, Virginia.
[70] Holdaway, M. Stability of andalusite and the aluminum silicate phase diagrams. Am. J. Sci. 271 (1971) 97-131.